JB
Journals.ASM.org

Selection of *dinB* Alleles Suppressing Survival Loss upon *dinB* Overexpression in *Escherichia coli*

Ryan W. Benson,* Tiziana M. Cafarelli,* Thomas J. Rands,* Ida Lin, Veronica G. Godoy

Department of Biology, Northeastern University, Boston, Massachusetts, USA

***Escherichia coli* strains overproducing DinB undergo survival loss; however, the mechanisms regulating this phenotype are poorly understood. Here we report a genetic selection revealing DinB residues essential to effect this loss-of-survival phenotype. The selection uses strains carrying both an antimutator allele of DNA polymerase III (Pol III) α-subunit (*dnaE915*) and either chromosomal or plasmid-borne *dinB* alleles. We hypothesized that *dnaE915* cells would respond to DinB overproduction differently from *dnaE*$^+$ cells because the *dnaE915* allele is known to have an altered genetic interaction with *dinB*$^+$ compared to its interaction with *dnaE*$^+$. Notably, we observe a loss-of-survival phenotype in *dnaE915* strains with either a chromosomal catalytically inactive *dinB*(*D103N*) allele or a low-copy-number plasmid-borne *dinB*$^+$ upon DNA damage treatment. Furthermore, we find that the loss-of-survival phenotype occurs independently of DNA damage treatment in a *dnaE915* strain expressing the catalytically inactive *dinB*(*D103N*) allele from a low-copy-number plasmid. The selective pressure imposed resulted in suppressor mutations that eliminated growth defects. The *dinB* intragenic mutations examined were either base pair substitutions or those that we inferred to be loss of function (i.e., deletions and insertions). Further analyses of selected novel *dinB* alleles, generated by single-base-pair substitutions in the *dnaE915* strain, indicated that these no longer effect loss of survival upon overproduction in *dnaE*$^+$ strains. These mutations are mapped to specific areas of DinB; this permits us to gain insights into the mechanisms underlying the DinB-mediated overproduction loss-of-survival phenotype.**

All cells accumulate DNA damage that, if left unrepaired, will stall DNA replication due to the inability of high-fidelity DNA polymerases (Pol) to use lesion-containing DNA as templates, a potentially lethal event (1). To ensure survival, *Escherichia coli* responds to replication fork stalling by upregulating the expression of the SOS-regulated genes (1–3), among which are specialized low-fidelity DNA polymerase genes. These polymerases can perform translesion synthesis (TLS), consisting of both insertion opposite to and elongation from DNA lesions on the template strand (4). TLS can result in elevated mutagenesis. In fact, data suggest that mutations responsible for resistance to several classes of antibiotics require TLS DNA polymerases (5–8). Moreover, these DNA polymerases appear to play a role in the development of disorders such as cancer in metazoans (9–12).

E. coli strains lacking the *dinB* gene (Δ*dinB*), encoding DinB (DNA Pol IV), one of the TLS DNA polymerases, are sensitive to nitrofurazone (NFZ) and 4-nitroquinoline-1-oxide (4-NQO) (13–15), reagents that generate persistent DNA lesions on the N^2 group of deoxyguanine (N^2-dG), as well as alkylating agents such as methyl methanesulfonate (MMS) (14, 16). Moreover, strains overproducing DinB undergo survival loss. It has been proposed that this is the result of lethal double-strand DNA breaks due to increased insertion of a damaged nucleotide (e.g., 8-oxo-dG) into DNA by DinB (17). Alternatively, it could be due to displacement of the catalytic subunit of the replicative DNA polymerase (Pol IIIα) from replication forks by the increased levels of DinB (18, 19).

Notably, *in vitro* DinB displaces Pol IIIα from other essential replication components (the processivity factor, β-clamp, and/or the DnaB helicase) at physiological concentrations of these proteins (18, 20). The displacement of Pol IIIα and further binding of DinB to these proteins would slow or even interrupt DNA replication (20). However, the molecular details of these events are mostly unknown, especially regarding the role of DinB and the specific residues that mediate displacement and binding between DinB and other replicative proteins.

We set up a genetic system that would permit us to gain insights into the DinB-mediated survival loss *in vivo*. The genetic system is composed of strains with both an antimutator *dnaE* allele (*dnaE915*) (21), encoding a variant of the replicative DNA polymerase active subunit, Pol IIIα(915), and the wild-type *dinB* (*dinB*$^+$) or the catalytically inactive *dinB*(*D103N*) allele. Pol IIIα(915) is an antimutator either because it synthesizes DNA slower than the native replicative DNA polymerase active subunit, DNA Pol IIIα (21, 22), or because it might inhibit low-fidelity DNA synthesis by TLS DNA polymerases, specifically DinB (23). Its antimutator activity is also dependent upon another TLS DNA polymerase, DNA Pol II, which likely prevents mutagenesis generated by DinB (24). This genetic system has permitted us to discover key DinB residues that mapped to specific areas of DinB, allowing us to gain insights into the mechanisms underlying the DinB-mediated overproduction loss-of-survival phenotype.

Received 21 April 2014 **Accepted** 6 June 2014

Published ahead of print 9 June 2014

Address correspondence to Veronica G. Godoy, v.godoycarter@neu.edu.

* Present address: Ryan W. Benson, Department of Microbiology, The Forsyth Institute, Cambridge, Massachusetts, USA; Tiziana M. Cafarelli, Center for Cancer Systems Biology, Dana-Farber Cancer Institute, and Department of Genetics, Harvard Medical School, Boston, Massachusetts, USA; Thomas J. Rands, Department of Molecular and Cell Biology, Brandeis University, Waltham, Massachusetts, USA.

Supplemental material for this article may be found at http://dx.doi.org/10.1128/JB.01782-14.

doi:10.1128/JB.01782-14

MATERIALS AND METHODS

Bacterial strains, plasmids, and other reagents. The parental strain used in this work is *E. coli* P90C with *dinB*$^+$ or its alleles (25), and MG1655 (26). All strains constructed in this report are isogenic to either P90C or MG1655. The low-copy-number plasmids we use are derivatives of pYG768 (27) with *dinB*$^+$ or its alleles. The overexpression vector used is pBAD18 (28) with either *dinB*$^+$ or its alleles. Bacterial strains, plasmids, and oligonucleotide sequences are listed in Table S1 in the supplemental material. All *dinB* alleles (see Table S1) were generated using CpG-methylase (New England BioLabs) and the GeneTailor site-directed mutagenesis system (Life Technologies) (14) using the *dinB* low-copy-number plasmid pYG768 (27) as template. *dinB* alleles were introduced into the pBAD18 arabinose-inducible overexpression vector (28) using standard recombinant DNA techniques with inserts containing XbaI and KpnI restriction sites. Plasmids were introduced into $CaCl_2$ chemically competent cells by transformation (29). P1 transduction (29) was used to move alleles between chromosomes of different *E. coli* strains. Ampicillin (Amp; Sigma) was used at 200 μg/ml unless indicated otherwise. The DNA-damaging agents used in this report are methyl methanesulfonate (MMS; Acros Organics), nitrofurazone (NFZ; Sigma), ciprofloxacin (Cip; Sigma), and UV irradiation (254 nm); the concentrations or intensities are shown in the respective figure legends. Glucose (0.2%) M9 minimal medium is supplemented with Casamino Acids (0.3%) except where noted otherwise. In all data where statistical significance between indicated samples (raw *P* values) is shown, the *t* test was used. Mutations were verified by DNA sequencing, which was carried out at the Tufts University Core Facility in Boston, MA.

Electrophoretic mobility shift assay (EMSA). Protein-DNA binding reaction mixtures were incubated in 20 μl of a 1× reaction buffer (50 mM HEPES [pH 7.5], 150 mM KCl) at 30°C for 35 min. Increasing amounts (15, 35, or 70 pmol) of native recombinant DinB and 0.5 pmol of DNA were used per reaction. The DNA used in these reactions is a primer-template junction containing a 5′ HEX (hexachlorofluorescein) fluorescently labeled primer (Integrated DNA Technologies [IDT]) and a complementary template containing either a stable alkylation lesion analogue, 3-deaza-3-methyladenine (30) (IDT) or an unmodified adenine (Eurofins MWG Operon). These DNA-protein mixtures were separated by electrophoresis on a 6% native polyacrylamide gel (0.5× Tris-borate-EDTA [TBE], 0.01 μg/ml bovine serum albumin [BSA]) at 65 V. The gel bands were visualized on a Typhoon 8600 phosphorimager from Amersham and quantified with ImageJ software (NIH).

Visualization of synthetic sick cells. The catalytically inactive plasmid-borne *dinB* allele, p*dinB*(*D103N*), was introduced into chemically competent *dnaE915* cells by transformation. After 19 to 22 h of incubation at 37°C, colonies were photographed at low magnification (×40) with a Nikon SMZ800 microscope. To visualize cells, colonies were resuspended in an isotonic solution and either of the following dyes was added: DAPI (4′,6-diamidino-2-phenylindole; an indication of live cells; 1 μg/ml; Sigma) or propidium iodide (an indication of dead cells; 1×; Life Technologies). Cells were incubated for 15 min at room temperature in the dark. One microliter of the cell suspension was added to an agarose pad on a microscope slide and visualized at ×1,000 on a fluorescence microscope (Leica DM5000B). To determine the percentage of cells undergoing SOS induction, we used a chromosomal reporter in which the SOS-regulated *sulA* gene promoter is fused to green fluorescent protein (GFP; Pr-*sulA*-GFP) (31). If the SOS gene network is induced, the GFP reporter fluoresces. DAPI was chosen to assess live cells instead of green SYTO-9 to allow for simultaneous determination of GFP fluorescence (i.e., SOS induction). The exposure times for DAPI (70 milliseconds), propidium iodide (50 milliseconds), and GFP (199 milliseconds) were constant throughout the experiments.

Quantification of gene expression. Ten thousand *dnaE915*/p*dinB*(*D103N*) cells coming from colonies with an altered morphology and with a chromosomal *sulA* promoter-GFP fusion (Pr-*sulA*-GFP) (31) were analyzed with a fluorescence-activated cell sorter (FACS; BD FACSAria II). SOS induction is defined as cells with fluorescence greater than that of *dnaE*$^+$ cells carrying the vector under the same conditions ($>10^2$). The value is chosen because values equal to or lower than 10^2 are what we find to be low/basal levels of SOS induction in *dnaE*$^+$ strains carrying the vector or any plasmid-borne *dinB* alleles.

Isolation of mutations that suppress *dinB*-dependent loss of survival. p*dinB*(*D103N*) was introduced into chemically competent *dnaE915* cells by transformation. To determine CFU/colony, independent colonies were resuspended in an isotonic solution, serially diluted, and deposited on appropriate plates. Strains with suppressors were identified due to the cells' ability to grow to saturation after approximately 20 h of incubation. Plasmids were purified (Qiagen's plasmid Miniprep kit) from cultures of suppressor colonies, and both the promoter and *dinB*(*D103N*) open reading frame were sequenced. Similar procedures were carried out for Δ*dinBdnaE915*/p*dinB*$^+$ strains that were no longer hypersensitive upon MMS treatment.

***In vitro* DNA polymerase primer extension assays.** Native recombinant DinB and its variants were purified as before (32). The DNA used in these reactions is a primer-template junction containing a 5′ HEX fluorescently labeled primer and a complementary template containing either a stable alkylation lesion analogue, 3-deaza-3-methyladenine, or an unmodified adenine. Reaction mixtures included 0.25 pmol of template DNA with 0.025, 0.125, 0.25, or 12.5 pmol of DinB, DinB(F292Y), or DinB(V7G) per reaction. Reactions were initiated by addition of enzyme, reaction mixtures were incubated at 37°C, and reactions were quenched by stop/loading dye after 10 min. Translesion DNA synthesis is measured as the ability of DinB or its derivatives to add nucleotides to the labeled primer using either lesion-containing or undamaged DNA templates. We used a "standing start" assay (13) in which the first nucleotide DinB adds to the primer is the one opposite to the lesion on the template. Then the DNA polymerase can continue DNA synthesis past the lesion. DinB adds one nucleotide at a time to the labeled primer (13), resulting in a ladder of DNA fragments that are different by one nucleotide in length. The newly synthesized end-labeled DNA is separated in a 10% denaturing polyacrylamide gel. These were visualized on a Typhoon 8600 phosphorimager from Amersham and quantified with ImageJ software (NIH). Statistical significance between samples was determined with the *t* test.

Assay to measure loss of survival due to DinB overproduction. DinB variants were overproduced from pBAD18 (28) with L-arabinose (0.2%) by following the protocol of Uchida et al. (18). Exceptions are the resuspension buffer (1× M9 salts) and M9 minimal medium supplemented with Casamino Acids that we used in these experiments. Aliquots were removed at the times indicated in the figures, serially diluted, plated on rich medium with 0.2% glucose, and incubated at 37°C. Amp was added to all growth media to ensure plasmid retention. The relative levels of DinB, DinB(F292Y), and DinB(V7G) in the Δ*dinB dnaE915* strain were determined using immunoblotting, as described before (32).

Circular dichroism (CD) spectroscopy. The secondary structures of DinB and DinB(F292Y) were analyzed as described before (32) using a Jasco J-715 spectropolarimeter. The spectrum of each sample was determined six times at wavelengths from 240 nm to 200 nm, and the data were analyzed using the CDPro software package and the CONTIN/LL algorithm.

RESULTS

The *dnaE915* allele sensitizes strains with a catalytically inactive chromosomal *dinB* allele to DNA damage treatment. We compared the survival of a *dnaE915* strain carrying a chromosomal catalytically inactive *dinB* allele, *dinB*(*D103N*) (14, 33), to that of an isogenic strain lacking the *dinB* gene upon treatment with methyl methanesulfonate (MMS) or nitrofurazone (NFZ) (Fig. 1A). We chose MMS and NFZ because these DNA-damaging agents generate lesions that are bypassed by DinB (13, 14, 16). We find that the *dnaE915* allele sensitizes the *dinB*(*D103N*) strain to treatment with MMS or NFZ as shown in Fig. 1A, whereas this

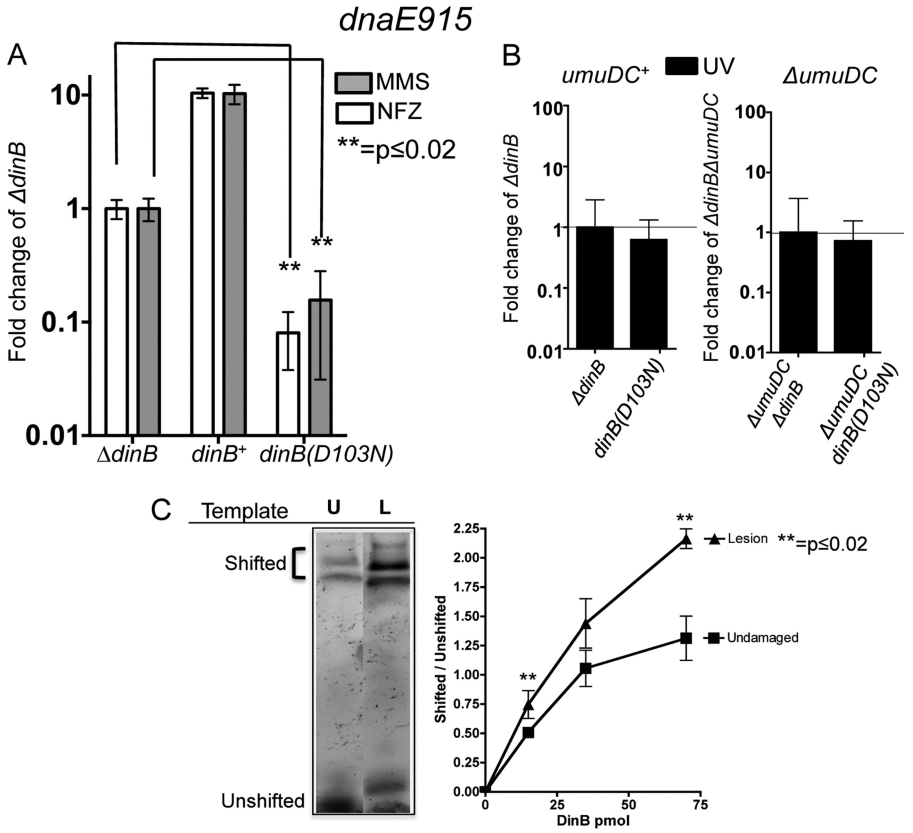

FIG 1 DNA damage treatment results in survival loss only in strains with both chromosomally encoded antimutator *dnaE915* and catalytically inactive *dinB*(*D103N*) alleles. (A) Treatment with either methyl methanesulfonate (MMS; 7.5 mM) or nitrofurazone (NFZ; 7.5 μM) of *dnaE915* strains with the chromosomal catalytically inactive *dinB* allele [*dinB*(*D103N*)] results in hypersensivity to these DNA damage reagents. Fold changes were calculated with respect to the survival of a *dnaE915* strain with a chromosomal deletion of *dinB* (Δ*dinB*) in NFZ ($1.4 \times 10^8 \pm 1.5 \times 10^7$ CFU/ml) or in MMS ($7.5 \times 10^7 \pm 2 \times 10^6$ CFU/ml). (B) Strains with chromosomal alleles *dnaE915* and Δ*dinB* and with *dnaE915* and *dinB*(*D103N*) equally survive UV treatment (~55 J/m^2) independent of the *umuDC* operon encoding DNA Pol V. Fold changes in this case were calculated based on UV treatment of *dnaE915* Δ*dinB* ($3 \times 10^8 \pm 3 \times 10^7$ CFU/ml) or Δ*umuDC dnaE915* Δ*dinB* ($3 \times 10^7 \pm 5 \times 10^6$ CFU/ml) strains. Error bars represent the standard deviations of the means from analyses of at least 3 independent isolates. (C) DinB prefers lesion-containing DNA. An electrophoretic mobility shift assay (EMSA) reveals that DinB preferentially binds to 3-deaza-3-methyl-adenine lesion-containing DNA (L) relative to undamaged DNA (U). Seventy-picomole DinB and 0.025-pmol DNA are shown. The lanes shown are from the same gel and have been electronically placed next to each other to directly compare the differences. The ratio of shifted (bound) to unshifted (unbound) DNA upon addition of the indicated concentrations of DinB is shown. Error bars represent the standard deviations of the means from analyses of at least 3 replicates. The band directly above the unshifted band in the L lane was not included in the quantification because we cannot consistently detect it. Band intensity was quantified using ImageJ (NIH).

increased-sensitivity phenotype is not seen in *dnaE*$^+$ strains, where *dnaE*$^+$ *dinB*(*D103N*) and *dnaE*$^+$ Δ*dinB* strains survive NFZ or MMS treatment equally well (14).

Next, we treated this strain with UV light, an agent that forms lesions that are not bypassed by DinB (1). We determined if there is a difference in survival between UV-treated isogenic strains without *dinB* (*dnaE915* Δ*dinB*) and a strain with a catalytically inactive *dinB* allele, the *dnaE915 dinB*(*D103N*) strain. Untreated strains survive equally well. We find no difference in UV survival between *dnaE915* Δ*dinB* and *dnaE915 dinB*(*D103N*) strains (Fig. 1B). However, these data could be explained by DNA Pol V outcompeting DinB(D103N) at the stalled replication fork due to DNA Pol V's ability to bypass UV lesions (1). We constructed strains lacking the *umuDC* genes, encoding DNA Pol V [Δ*umuDC dnaE915* Δ*dinB* and Δ*umuDC dnaE915 dinB*(*D103N*)], and UV irradiated them. As above, untreated strains show no survival loss. We find that the Δ*umuDC dnaE915 dinB*(*D103N*) strain has no difference in UV survival (Fig. 1B) compared to the Δ*umuDC dnaE915* Δ*dinB* strain, suggesting that the MMS or NFZ hypersensitivity (Fig. 1A) observed in the *dnaE915 dinB*(*D103N*) strain is DinB specific.

We then wondered whether the lesion might serve as a DinB targeting signal, which would effectively increase DinB's local concentration at the replication fork. To examine this possibility, we conducted an electrophoretic mobility shift assay (EMSA) to compare the relative affinities of DinB for template DNA containing adenine or the alkylation lesion analogue, 3-deaza-3-methyladenine. We hypothesized that DinB might bind better to templates containing this alkylation lesion than to undamaged templates. Consistent with this hypothesis, we find that DinB appears to have a preference for MMS lesion-containing DNA (Fig. 1C).

Taking the data together, we have observed that the *dnaE915 dinB*(*D103N*) strain is sensitized to reagents producing lesions bypassed by DinB (NFZ or MMS) at chromosomal intracellular concentrations of DinB(D103N). Moreover, DinB binds better to alkylation lesion-containing DNA than to undamaged DNA, sug-

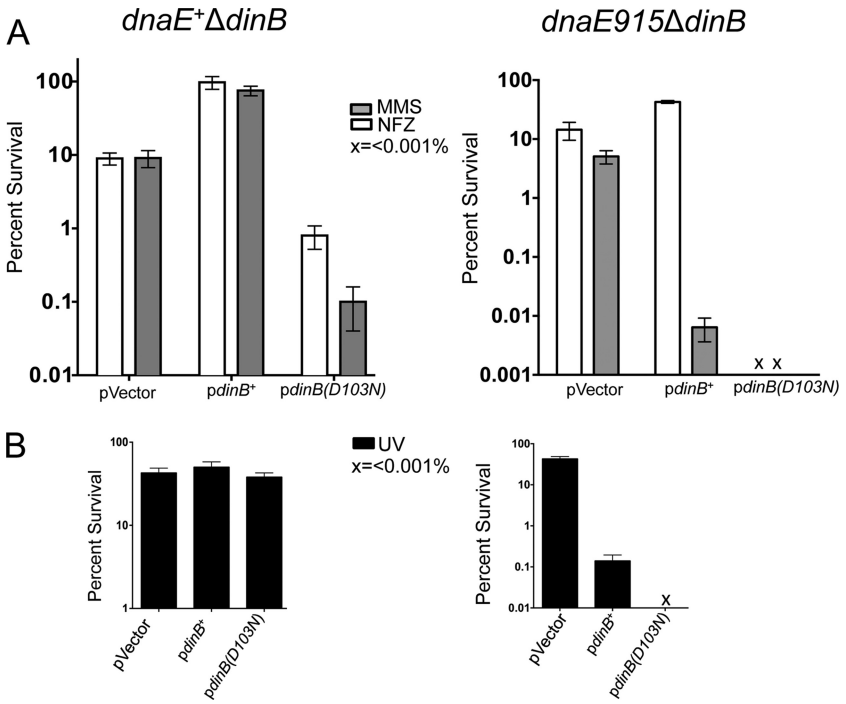

FIG 2 The plasmid-borne *dinB*$^+$ mediates survival loss only in *dnaE915* strains. (A) The *dnaE*$^+$ Δ*dinB* strain with the plasmid-borne *dinB*$^+$ (p*dinB*$^+$) is resistant to MMS (7.5 mM) or NFZ (7.5 μM) compared to the strain carrying the vector. The *dnaE915* Δ*dinB*/p*dinB*$^+$ strain is more resistant to NFZ than cells carrying the vector; however, survival loss is evident in the Δ*dinB dnaE915* strain carrying the plasmid-borne p*dinB*$^+$ or the catalytically inactive p*dinB*(*D103N*) allele upon MMS treatment (7.5 mM). (B) Plasmid-borne p*dinB*$^+$ does not affect survival in the *dnaE*$^+$ Δ*dinB* upon UV treatment. UV irradiation (~40 J/m^2) results in survival loss in the *dnaE915* Δ*dinB* strain carrying p*dinB*$^+$ or p*dinB*(*D103N*). x, <0.001% survival. The percent survival is calculated based on the CFU/ml values for the untreated cells, which are similar for all strains (~1 × 10^9 CFU/ml) except the *dnaE915* Δ*dinB*/p*dinB*(*D103N*) strain, which has ~1 × 10^8 CFU/ml. Error bars represent the standard deviations of the means from the analysis of at least 3 independent isolates.

gesting a mechanism to increase DinB local concentration at the replication fork.

***dnaE915* strains expressing plasmid-borne *dinB*$^+$ are sensitized to DNA damage treatment.** We then tested whether somewhat higher intracellular concentrations of DinB in a *dnaE915* strain would also result in survival loss upon DNA damage treatment. To that end, *dinB*$^+$ was expressed from its own DNA damage-inducible promoter on a low-copy-number plasmid previously shown by others (27, 34) to express *dinB*$^+$ at 5- to 10-times-higher levels than the chromosome (i.e., between 1,250 and 2,500 molecules per cell in uninduced cells and an ~10-fold increase to 25,000 molecules upon SOS induction).

Surprisingly, we find that expression of *dinB*$^+$ from this plasmid results in MMS-induced survival loss or MMS hypersensitivity, compared to the *dnaE915* Δ*dinB* strain with the vector (Fig. 2A). This is striking, considering that the same plasmid-borne *dinB*$^+$ restores MMS resistance to *dnaE*$^+$ Δ*dinB* cells (Fig. 2A) (14, 16). Thus, the higher-than-chromosomal intracellular concentration of DinB effects survival loss in the *dnaE915* strain. To exclude the possibility that our findings are unique to the P90C strain, we recreated this phenotype in *E. coli* MG1655 with similar results (see Fig. S1A in the supplemental material).

The *dnaE915* Δ*dinB*/p*dinB*$^+$ strain was also treated with NFZ as a comparison (Fig. 2A). However, the *dinB*$^+$-dependent survival loss phenotype is specific to MMS treatment. Since MMS is a stronger inducer of the SOS gene network than NFZ (14), we thought the observed MMS-induced survival loss could be dependent on a higher DinB intracellular concentration resulting from SOS induction or on other SOS-induced genes. It is also plausible that cell elongation occurring upon SOS induction (1) could result in lower CFU counts upon MMS treatment because even if all cells within the filament grow, they will be physically too close to produce independent colonies. Since cell elongation during SOS induction is *sulA* dependent, we tested whether isogenic cells lacking *sulA* (Δ*sulA dnaE915* Δ*dinB*/p*dinB*$^+$) were MMS hypersensitive. We find this is the case (see Fig. S2A in the supplemental material). Therefore, it appears that the hypersensitive phenotype is specific to effects on DNA damage metabolism and not to inhibition of cell division.

We also find that the MMS-induced survival loss effected by p*dinB*$^+$ is eliminated in isogenic strains that are SOS deficient because they either lack *recA* (Δ*recA dnaE915* Δ*dinB*/p*dinB*$^+$) or have an uncleavable *lexA* allele (*lexA3 dnaE915* Δ*dinB*/p*dinB*$^+$) (see Fig. S3A in the supplemental material). We next determined if the observed hypersensitivity was MMS specific or if other equally potent inducers of the SOS gene network also produced hypersensitivity. To do this, we UV irradiated a *dnaE915* Δ*dinB* strain expressing p*dinB*$^+$ or treated it with ciprofloxacin (Cip; 0.16 μg/ml) to induce the SOS network (1, 14). We find that these cells are indeed sensitized to UV (Fig. 2B) or Cip (data not shown), unlike the isogenic *dnaE*$^+$ strain (Fig. 2B and data not shown). From these data, we infer that the observed DinB toxicity in the *dnaE915* strain effecting survival loss upon MMS treatment is due to higher intracellular concentrations of DinB upon SOS induction.

The *dnaE915* strain expressing a plasmid-borne catalytically inactive DinB(D103N) allele survives poorly. We then discov-

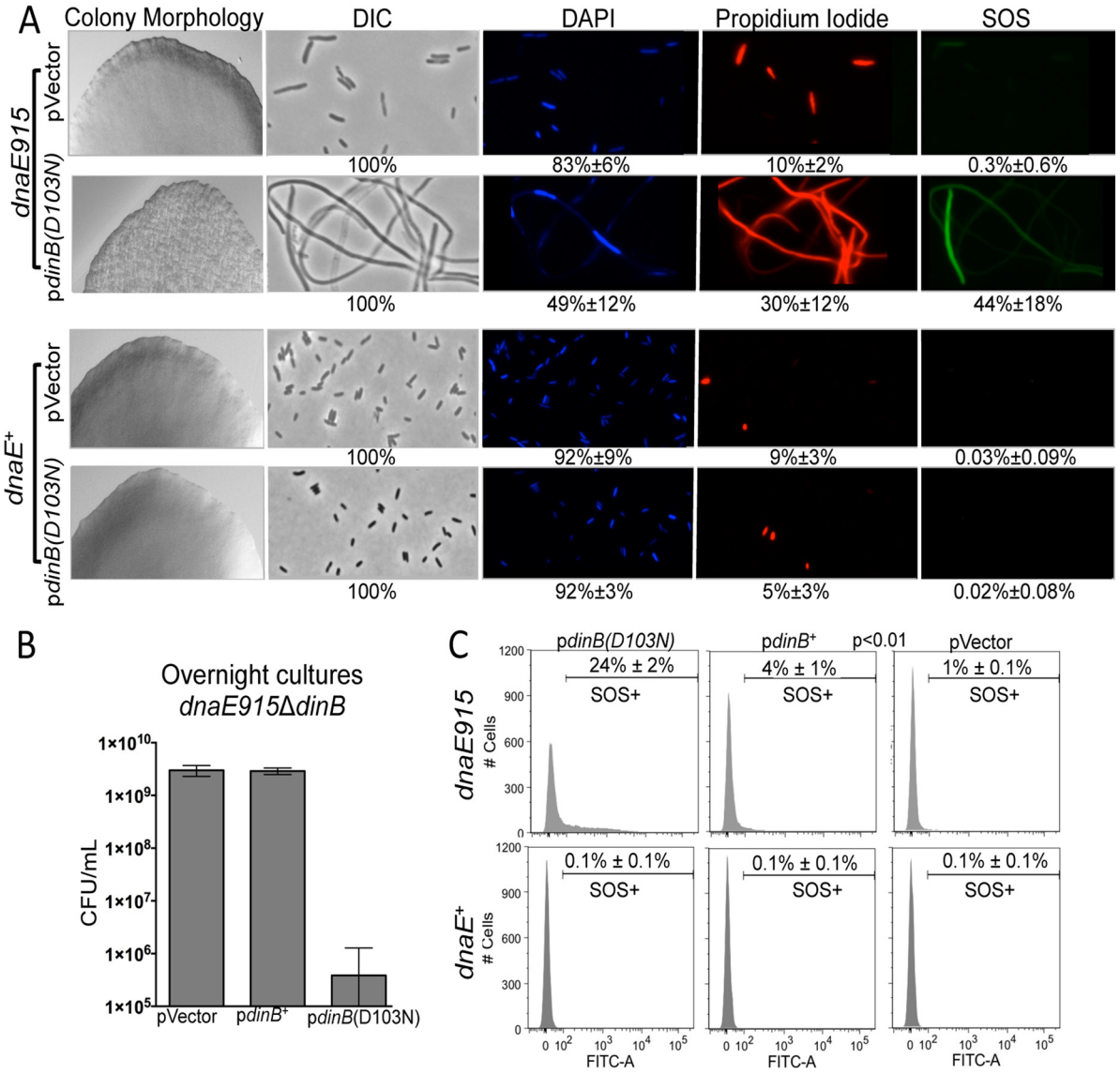

FIG 3 Antagonistic genetic interactions between the *dnaE915* and plasmid-borne *dinB*(*D103N*) alleles results in synthetic sickness in the absence of DNA damage treatment. (A) Colonies formed by *dnaE915* Δ*dinB*/p*dinB*(*D103N*) cells have altered morphology. Representative sections of colonies of *dnaE915* Δ*dinB* cells with pVector (normal morphology) and p*dinB*(*D103N*) (synthetically sick) compared to the colonies of isogenic *dnaE*$^+$ Δ*dinB* cells with the same plasmids (normal morphology) at ×40 are shown. The morphology (differential interference contrast [DIC]), viability (DAPI, live; propidium iodide, dead), and SOS induction measured as GFP expression from an SOS regulated promoter (Pr-*sulA*-GFP) were assessed by fluorescence microscopy at ×1,000 in cells from the respective colonies. *dnaE915* Δ*dinB*/p*dinB*(*D103N*) cells are elongated, fewer of them survive, and the SOS is induced in a fraction of cells. *dnaE915* cells carrying the vector or isogenic *dnaE*$^+$ strains with either vector or p*dinB*(*D103N*) do not experience survival loss and SOS induction. The different features were quantified as shown at the bottom of each representative microscope field from counting at least 500 cells from different fields of at least 3 independent colonies. (B) Cultures started from *dnaE915* Δ*dinB*/p*dinB*(*D103N*) colonies do not reach saturation after 24 h in LB medium and have ~1,000-fold fewer CFU/ml than cultures of *dnaE915* Δ*dinB* cells carrying either the vector or p*dinB*$^+$. Error bars represent standard deviations of the means from at least 5 independent isolates. (C) SOS induction of cells within colonies was determined using a fluorescence-activated cell sorter (FACS). Approximately 25% of cells in Pr-*sulA*-GFP *dnaE915* Δ*dinB*/p*dinB*(*D103N*) colonies [p*dinB*(*D103N*)] with the synthetically sick morphology undergo SOS induction. A small population (4%) of Pr-*sulAp*-GFP *dnaE915* Δ*dinB*/p*dinB*$^+$ (p*dinB*$^+$) cells are SOS induced. As in panel A, there is negligible SOS induction in Pr-*sulA*-GFP *dnaE915* Δ*dinB*/pVector (pVector) or Pr-*sulA*-GFP *dnaE*$^+$ Δ*dinB* cells with any of the DinB variants tested. SOS induction is considered as FITC-A values of $>10^2$. The measurements are the result of 10,000 cells analyzed from 3 independent colonies of each strain.

ered that the expression of the plasmid-borne catalytically inactive *dinB* allele, p*dinB*(*D103N*), results in aberrant colony morphology in the absence of DNA damage treatment only in a *dnaE915* Δ*dinB* strain (Fig. 3A). This morphology is unique to the *dnaE915* strain with the plasmid-borne p*dinB*(*D103N*) and is absent in the isogenic strain with the vector or in their *dnaE*$^+$ counterparts (Fig. 3A). In addition, the *dnaE915* Δ*dinB*/p*dinB*(*D103N*) colonies have fewer CFU/colony [$\sim 1 \times 10^7$ for the p*dinB*(*D103N*) strain versus $\sim 1 \times 10^8$ for the pVector strain], and cultures of these colonies do not reach saturation in rich liquid medium after 20 h of incubation at 37°C compared to cultures from colonies containing only the vector (Fig. 3B). Since the aberrant colony morphology is not

observed in the *dnaE915* strain with the vector alone (Fig. 3A) or in *dnaE*$^+$/p*dinB*(*D103N*) cells (Fig. 3A) (13, 14), we infer that this phenotype is synthetic. The allele combination results in less-than-expected fitness, and because the combination is not lethal, we use the synthetic sick terminology (35).

Next, we used microscopy to test whether the *dnaE915* Δ*dinB*/p*dinB*(*D103N*) aberrant-morphology colonies contain dead cells, as the CFU determination suggests. We used DAPI to stain live cells and propidium iodide to stain dead cells. We find that a large fraction of cells from the synthetic sick colonies are dead and/or elongated (Fig. 3A), unlike *dnaE915* Δ*dinB*/pVector or *dnaE*$^+$ Δ*dinB*/p*dinB*(*D103N*) colonies (Fig. 3A). Notably, cells from Δ*sulA dnaE915* Δ*dinB*/p*dinB*(*D103N*) colonies display the synthetic sick phenotypes (see Fig. S2 in the supplemental material). Like the *sulA*$^+$ isogenic strains, colonies have fewer CFU than colonies carrying the vector [$\sim 1 \times 10^7$ CFU for p*dinB*(*D103N*) colonies versus $\sim 1 \times 10^8$ for pVector colonies] and most colonies do not reach saturation in rich liquid medium upon subculture (see Fig. S2B). Additionally, cell elongation is reduced in the absence of *sulA* (see Fig. S2C); however, it is not completely abolished, indicating that the observed elongation is only partially dependent on *sulA*. Thus, the *dnaE915* Δ*dinB*/p*dinB*(*D103N*) strain is indeed sick; aberrantly shaped colonies have more dead and/or elongated cells than colonies carrying the vector, and the SOS network is induced in a fraction of the population without DNA damage treatment (Fig. 3A; see below).

As expected, *dnaE915* Δ*dinB*/p*dinB*(*D103N*) cells are highly sensitive to DNA damage treatment. In fact we find less than 0.001% survival upon treatment with MMS, NFZ, or UV (Fig. 2A and B). Therefore, the combination of the *dnaE915* allele with the *dinB*(*D103N*) allele resulted in either sickness in the absence of or lethality upon DNA damage treatment.

The p*dinB*(*D103N*) plasmid was also introduced into *dnaE915* Δ*dinB* MG1655 cells. We find the aforementioned antagonistic genetic interaction between *dnaE915* and plasmid-borne *dinB*(*D103N*), again suggesting that our findings are strain independent (see Fig. S1B in the supplemental material). Given these results, we chose to further study the *dnaE915* Δ*dinB*/p*dinB*(*D103N*) strain because of this robust phenotype. Furthermore, any growth defects observed with the catalytically inactive *dinB*(*D103N*) allele are independent of DinB's DNA synthesis or bypass activities and are likely dependent on protein-protein or protein-DNA interactions.

The β-clamp processivity factor binding motif is required in DinB(D103N) to effect synthetic sickness. We wanted to determine if the interactions that we observe are the product of events occurring through interactions with other replication proteins, such as the β-clamp processivity factor, possibly at the replication fork. We used an allele of *dinB*(*D103N*) lacking the coding sequence for the last five carboxy-terminal amino acids [*dinB*(*D103N*)Δβ] (14), which make up the β-clamp binding motif (36). This was introduced by transformation into *dnaE915* cells. Notably, synthetic sickness is absent in this strain (see Fig. S4 in the supplemental material). The requirement for the β-clamp binding motif to observe the growth defects (or CFU loss) described here suggests that DinB(D103N) might be localized at the replication fork, consistent with an increase in DinB(D103N) (and likely DinB) local concentration. Once at the replication fork, the catalytically inactive derivative would stall DNA replication independent of DNA damage treatment, which would in turn induce the SOS gene network (1). Therefore, we would predict that *dnaE915* Δ*dinB*/p*dinB*(*D103N*) cells have measurable SOS induction.

To measure SOS induction, we introduced an SOS-inducible reporter gene fusion (31) onto the chromosome of *dnaE915* by transduction. This reporter consists of the DNA damage response *sulA* promoter gene fused to green fluorescent protein (Pr-*sulA*-GFP). Since we observe the survival loss phenotype with no DNA damage treatment, the SOS induction could be due to DNA replication stalling independent of DNA damage, which is effected at the replication fork by the DinB(D103N) derivative. Possibly, though unlikely, SOS induction could be due to an increased load of endogenous lesions uniquely in this strain that are not bypassed by DinB(D103N). The readout for both of these is the same, i.e., fluorescence, as we cannot distinguish mechanistically what is happening at the fork since in both cases there will be replication stalling.

The fraction of cells that were SOS induced was measured using microscopy or a fluorescence-activated cell sorter (FACS). Through microscopy, we find increased SOS induction in cells from the Pr-*sulA*-GFP *dnaE915* Δ*dinB*/p*dinB*(*D103N*) synthetic sick colonies (mean ± standard deviation [SD], 44% ± 18%) (Fig. 3A) compared to cells in isogenic colonies with normal morphology (*dnaE915*/pVector or any *dnaE*$^+$ with any plasmid assayed here, <0.3%). Due to this low level of SOS induction in *dnaE*$^+$ cells in the absence of DNA damage, we define SOS-induced cells in the FACS assays as those with fluorescence higher than that of untreated *dnaE*$^+$ Δ*dinB* cells (i.e., 10^2). As with microscopy, cells resuspended from Pr-*sulA*-GFP *dnaE915* Δ*dinB*/p*dinB*(*D103N*) colonies have an elevated fraction of fluorescence (mean ± SD, ~24% ± 2%) compared to cells from colonies with the vector alone (1%) (Fig. 3C). A smaller fraction (4%) of cells of the isogenic strain with a plasmid-borne p*dinB*$^+$ (Pr-*sulA*-GFP *dnaE915* Δ*dinB*/p*dinB*$^+$) also undergo SOS induction in the absence of DNA damage, indicating that DinB alone might generate some level of replication stalling (Fig. 3C). We again find that all of the *dnaE*$^+$ Δ*dinB* strains have no SOS induction (Fig. 3C). Therefore, SOS induction likely arises from genetic interactions between DinB(D103N) (or to a lesser degree DinB) and *dnaE915* at the replication fork and in the absence of DNA damage treatment.

Notably, isogenic strains that are deficient for SOS induction (Δ*recA dnaE915* Δ*dinB* or *lexA3 dnaE915* Δ*dinB*) with p*dinB*(*D103N*) display the features associated with the synthetic sickness phenotype (see Fig. S3B and C in the supplemental material), although these phenotypes are not as robust. Importantly, this is unlike the p*dinB*$^+$-dependent loss of survival upon MMS or UV treatment, which requires SOS induction. It appears that survival loss mediated by DinB requires higher intracellular levels of the native protein than the catalytically inactive DinB(D103N). Because both plasmid-borne alleles are under the control of their native SOS-inducible promoter, p*dinB*$^+$ requires induction, while p*dinB*(*D103N*) effects survival loss phenotypes at basal levels.

We thought that the growth defects of the *dnaE915* Δ*dinB*/p*dinB*(*D103N*) strain could be dependent on growth rate. Thus, we deposited the *dnaE915* Δ*dinB*/p*dinB*(*D103N*) transformation mix onto minimal medium plates instead of LB, reasoning that the cells would grow slower and possibly experience overall less cellular stress. Unexpectedly, we find no colonies on these plates (see Fig. S5 in the supplemental material). Like the synthetic sick colony morphology on LB medium, this phenotype is absent both in

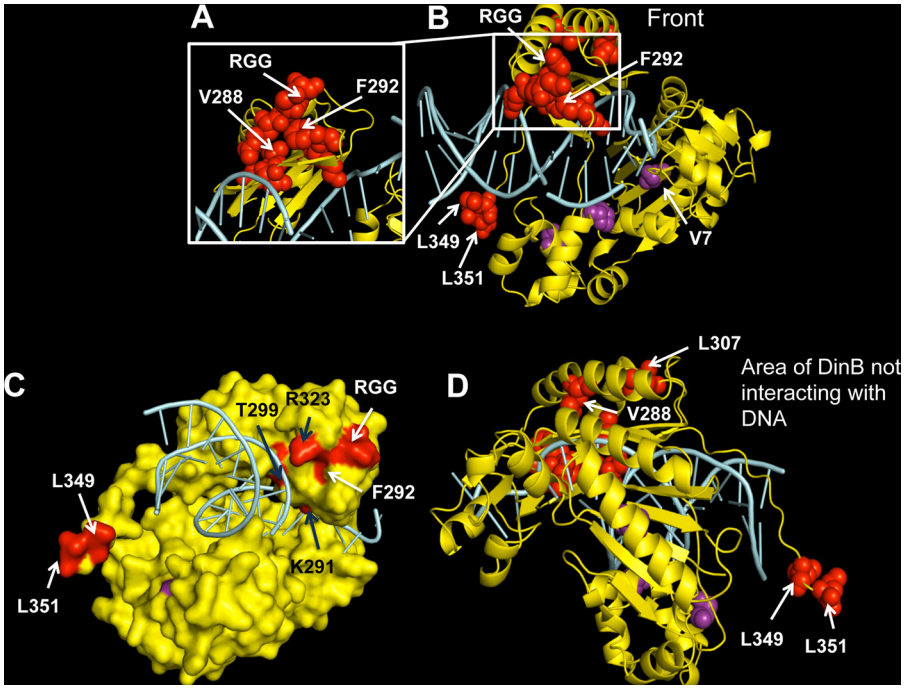

FIG 4 A diverse array of intragenic *dinB* mutations suppresses survival loss. Shown is a mapping of the suppressor mutations on the *in silico* model of the DinB tertiary structure. Amino acid changes resulting from base pair substitutions and a three-amino-acid (arginine, glycine, glycine [RGG]) duplication identified in our assay are depicted as red or purple spheres in the DinB ribbon rendering. DinB protein is colored yellow, and DNA is colored cyan. Mutated residues mentioned in this paper (valine [V] 7 or 288, phenylalanine [F] 292, leucine [L] 307, 349, or 351; the RGG duplication) are labeled on the structure. (A) A magnified view of the area of DinB containing most amino acid mutations (including V288G and F292 to tyrosine [Y]). (B) Front view, defined here as the face of the DNA polymerase in which the DNA is also visible. (C) Surface rendering of DinB with mutations colored red or purple. The F292 amino acid is predicted to be on the surface of the protein. Black arrows indicate residues that might be interacting with DNA. (D) Depiction of the area of DinB that does not interact with DNA, the opposite face of that shown in panel B, in which we found no mutations. Images were rendered with PyMOL (DeLano Scientific, San Carlos, CA, USA).

dnaE915 Δ*dinB* cells carrying the vector or p*dinB*$^+$ and isogenic *dnaE*$^+$ Δ*dinB* cells (data not shown). As before, we find that deletion of the DinB motif required for interactions with the β-clamp eliminates the loss-of-survival phenotype on minimal medium (see Fig. S5). We also find that the isogenic Δ*recA dnaE915* Δ*dinB*/p*dinB*(*D103N*) strain forms colonies on minimal medium (see Fig. S5), suggesting that either the induction of the SOS gene network or RecA is needed to observe this phenotype. These experiments suggest that the survival loss phenotype is independent of growth rate.

Synthetic sickness and DNA damage-induced survival loss are suppressed by mutations in p*dinB*(*D103N*) or p*dinB*$^+$. We observed that, upon subsequent culturing, the *dnaE915* Δ*dinB*/p*dinB*(*D103N*) strain grew to full saturation (see Fig. S6A in the supplemental material) and generated colonies of normal morphology. We surmised that this robust growth was the product of suppressor mutations.

Furthermore, we hypothesized that the MMS-induced survival loss in *dnaE915* Δ*dinB* cells with p*dinB*$^+$ could also be suppressed. We found that MMS hypersensitivity is abolished upon subculturing of MMS-treated colonies (see Fig. S6B in the supplemental material). In fact, several of the suppressor strains now displayed resistance to MMS (see Fig. S6B), similar to that observed for the *dnaE*$^+$ Δ*dinB*/p*dinB*$^+$ strain (14). Interestingly, all of these isolates except one (17 of 18 isolates; ~94%) survive NFZ treatment better than cells carrying the vector (see Fig. S6B; data not shown). This suggests that the DinB expressed in these suppressor strains has retained total or partial translesion synthesis activity and that the inability to effect MMS hypersensitivity is not the result of a nonfunctional protein.

Notably, though the synthetic sickness is evident in Δ*recA* or *lexA3* strains carrying p*dinB*(*D103N*), these cells fail to acquire full growth and normal colony morphology, unlike the SOS-proficient strains shown above (see Fig. S6A in the supplemental material), even after multiple subculture rounds (data not shown). This suggests that, although the induction of other SOS genes is not required for synthetic sickness, these genes are likely involved in generating mutations that suppress this phenotype.

To identify the suppressor mutations, we purified plasmids from *dnaE915* Δ*dinB*/p*dinB*(*D103N*) or *dnaE915* Δ*dinB*/p*dinB*$^+$ isolates that have lost either synthetic sickness or MMS hypersensitivity, respectively. Both the promoter and the *dinB*(*D103N*) or *dinB*$^+$ coding regions were sequenced. In this fashion, we identified various *dinB* intragenic suppressor mutations (Fig. 4 and Table 1). The mutations we find in p*dinB*(*D103N*) include point mutations ($n = 9$) and other rearrangements (Table 1). For example, we find, in addition to the D103N mutation, base pair substitutions at (L349 and L351 codons) or near (L307 codon) (Fig. 4 and Table 2) areas of the DinB gene that are important for interactions of DinB with the β-clamp processivity factor (36–38). For the p*dinB*$^+$ plasmids, mutations include an out-of-frame deletion resulting in a truncated protein downstream of D103 and two base

TABLE 1 Types of suppressor mutations

dinB intragenic mutation	Frequency (approx %) in *dnaE915* in:		
	MMS-treated Δ*dinB*/ p*dinB*$^+$ strain (n = 18)	Δ*dinB*/ p*dinB*(*D103N*) strain (n = 40)	ΔTLS p*dinB*(*D103N*) strain (n = 9)
None	83	40	11
Substitution mutation	11	23	33
Frameshift mutation	0	3	0
Duplication	0	13	0
Insertion sequence	0	3	0
Deletion	6	7	44
Rearrangement	0	3	0
Other	0	8	11

pair substitutions resulting in the F292Y or V7G variants (Tables 1 and 2; see Fig. S6B in the supplemental material).

Many of the mutations are localized to two specific areas of the protein (Fig. 4A and B, red or purple spheres). We surmise these areas might be important for either protein stability or represent an interface for interactions with either proteins or the DNA that generate the observed loss-of-survival phenotypes. Mapping the suppressor mutations onto an *in silico* structural DinB model reveals that many of the amino acids in these areas of DinB are likely either on the surface of the protein (Fig. 4C, white arrows) or in close proximity to the DNA (Fig. 4C, black arrows), further underscoring their possible importance in protein-protein or protein-DNA interactions. We found that base pair substitution suppressor mutations are absent from the area of the protein that does not interact with the DNA (Fig. 4D).

We hypothesized that the other specialized lesion bypass low-fidelity DNA polymerases (Pol II and Pol V) might be responsible for the base pair substitution suppressor mutations (1, 39). Thus, we used a *dnaE915* strain lacking the genes encoding all three TLS DNA polymerases (ΔTLS *dnaE915*), reasoning that this would reduce or eliminate base pair substitutions. Unexpectedly, we still find *dinB*(*D103N*) intragenic suppressor mutations that are the result of base pair substitutions in the absence of DNA damage in cells lacking TLS DNA polymerases (Table 1). Among these mutations is yet another independent V288G mutation (Table 2). We also find there is an increase in deletion mutations (44% compared to 7%) (Table 1), a mutation signature of Pol III (40). This demonstrates that the strong selective pressure of this genetic selection gives rise to suppressor mutations in the absence of DNA damage treatment, even in cells bearing only high-fidelity DNA polymerases (DNA Pol I and Pol III) and intact DNA damage response and repair systems.

Analyses of DinB derivatives suppressing survival loss. We then focused on the base pair substitution DinB suppressors, since these would permit us to gain insights into the noncatalytic areas of the DinB protein involved in the loss-of-survival phenotype. We infer that other classes of mutations (e.g., deletions, insertions, and large rearrangements) suppress survival loss because they result in a nonfunctional protein. Specifically, we elected to further analyze the *dinB*(*F292Y*) and *dinB*(*V7G*) alleles because they carry the sole base pair substitutions selected in *dinB*$^+$. In addition, we chose to study the base pair substitution in the *dinB*(*V288G*) allele from among the different base pair substitutions identified in the catalytically inactive *dinB*(*D103N*) allele because it arose independently in multiple isolates, underscoring its relevance in mediating survival loss. If the observed DinB-dependent growth defects [those found with either DinB or DinB(D103N)] are part of similar pathways, then suppressors arising in DinB should suppress DinB(D103N) and vice versa. Therefore, the F292Y or V7G mutations that were both originally found to be in p*dinB*$^+$ were introduced into p*dinB*(*D103N*) and the V288G mutation originally found in p*dinB*(*D103N*) was introduced into p*dinB*$^+$. We hypothesized these newly created plasmids should suppress any survival loss phenotype. We find that *dnaE915* Δ*dinB* cells bearing p*dinB*(*V288G*) behave as an isogenic strain carrying the vector, in which the MMS-dependent survival loss is absent (see Fig. S7A in the supplemental material). Likewise, *dnaE915* Δ*dinB* cells with p*dinB*(*D103N*) in addition to the F292Y or V7G mutation form colonies with normal morphology (see Fig. S7B).

To further understand whether the DinB suppressor mutations affect the structure and/or function of DinB in a *dnaE*$^+$ background, we chose the plasmids with a single base pair substitution in p*dinB*$^+$, encoding DinB(V288G), DinB(F292Y), or DinB(V7G), and studied *in vivo* TLS. This refers to the resistance of strains to MMS or NFZ treatment, which will occur only if these cells carry a functional form of the *dinB* gene. We find that *dnaE*$^+$ Δ*dinB* strains expressing the plasmid-borne *dinB*(*V288G*) survive as well as those with the vector alone, suggesting that the V288G mutation renders DinB nonfunctional. This mutation also impaired the purification of the DinB(V288G) protein, as this derivative is insoluble (data not shown).

Unlike expression of DinB(V288G), we find that either p*dinB*(*F292Y*) or p*dinB*(*V7G*) expression confers resistance to MMS or NFZ treatment in *dnaE*$^+$ Δ*dinB* cells, indicating that both variants have *in vivo* TLS activity (Fig. 5A). Perhaps these variants interact differently with replicative proteins or with the lesions themselves, compared to DinB. This could change the local concentration of DinB(F292Y) or DinB(V7G) at the replication fork to levels which would permit lesion bypass but which would not effect survival loss in *dnaE915*.

We purified DinB(F292Y) and DinB(V7G) and assessed their *in vitro* TLS activity. As before (32, 41), we used "standing start"

TABLE 2 List of *dinB* intragenic suppressor alleles

Allele	Missense mutation	Structure area[b]	Catalytic activity *in vivo*/*in vitro*	Allele no.[a]
dinB(*V7G*)	T to G	1	Yes/yes	*dinB68*
dinB(*P182L*)	C to T	1	NK[d]	*dinB69*
dinB(*S226R*)	A to C	1	NK	*dinB70*
dinB(*L266R*)	T to G	2	NK	*dinB71*
dinB(*V288G*)[c]	T to G	2	No/insoluble	*dinB72*
dinB(*K291E*)	A to G	2	NK	*dinB73*
dinB(*F292Y*)	T to A	2	Yes/yes	*dinB74*
dinB(*T299I*)	C to T	2	NK	*dinB75*
dinB(*L307Q*)	T to A	2	NK	*dinB76*
dinB(*R323C*)	C to T	2	NK	*dinB77*
dinB(*L349P*)	T to C	2	NK	*dinB78*
dinB(*L351S*)	T to C	2	NK	*dinB79*

[a] Allele numbers are assigned by the Coli Genetic Stock Center at Yale University.
[b] 1, area surrounding the catalytic core of the protein; 2, not catalytic area of the protein.
[c] The V228G amino acid substitution independently arose in multiple isolates.
[d] NK, not known.

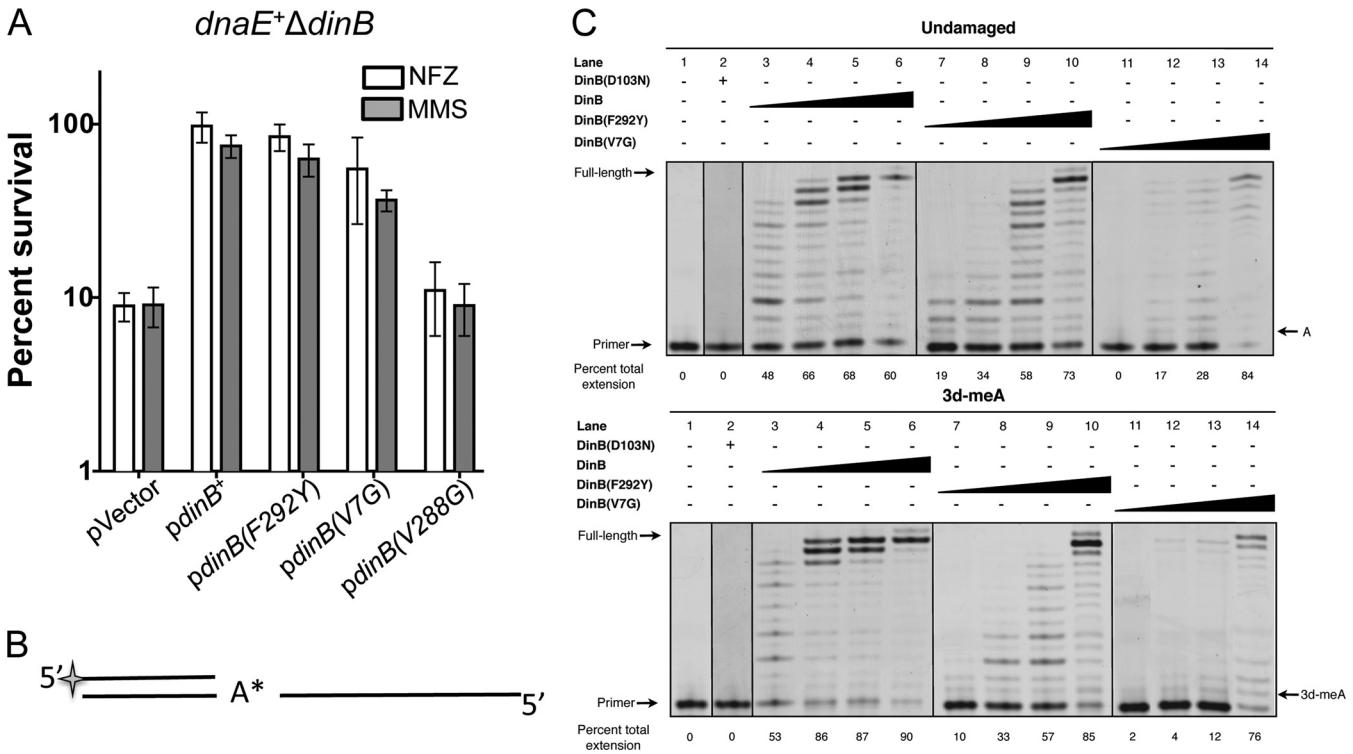

FIG 5 Examples of *dinB* growth arrest suppressor alleles that retain catalytic and lesion bypass activity *in vivo* and *in vitro*. (A) *dnaE*$^+$ Δ*dinB* cells with plasmids bearing wild-type *dinB*$^+$ or the *dinB*(*F292Y*), *dinB*(*V7G*), or *dinB*(*V288G*) suppressor alleles were treated with NFZ (7.5 μM) or MMS (7.5 mM) to determine *in vivo* TLS activity. *dnaE*$^+$ Δ*dinB* cells with p*dinB*(*F292Y*) or p*dinB*(*V7G*) survive better than cells with the vector. The percent survival is calculated based on the CFU/ml values for the untreated cells, which are similar for all strains (~1×10^9 CFU/ml). Error bars represent the standard deviations of the means from the analysis of at least 3 independent isolates. (B) Schematic of a standing start primer extension assay in which the first incorporated nucleotide is opposite the lesion. A* represents the HEX fluorophore. (C) Standing start DNA extension assays with 0.25 pmol of undamaged or lesion-containing templates (same as those shown in Fig. 1C) and titrations of DinB, DinB(F292Y), or DinB(V7G) (undiluted 12.5 pmol and dilutions of 1:50, 1:100, or 1:500). DinB, DinB(F292Y), and DinB(V7G) can insert a nucleotide opposite to and extend from an adenine (A) or 3-deaza-3-methyladenine (3-dMeA). At the undiluted concentration (lanes 6 and 10), both DinB and DinB(F292Y) preferentially replicate a lesion-containing template over an undamaged template ($P < 0.05$). In contrast, DinB(V7G) lacks a significant template preference ($P > 0.05$; lane 14). The catalytically inactive DinB(D103N) is unable to replicate either template (lane 2). The lanes shown are from the same gel and have been electronically placed next to each other to directly compare the differences.

assays (13, 32, 41), where the first nucleotide added to the primer is the one opposite to the template lesion (see Fig. 5B for a diagram), to determine the *in vitro* activity of the DinB variants compared to native DinB on undamaged or 3-methyladenine (3-meA) analogue-containing templates. DinB(F292Y) and DinB(V7G) have *in vitro* TLS activity (Fig. 5C), supporting our *in vivo* findings (Fig. 5A). We noticed that there is less-unextended primer in DinB reactions with a 3-meA analogue template compared to the reactions with the undamaged template, suggesting template preference. The same trend is observed in DinB(F292Y), although this appears less robust than in DinB. The quantified overall DNA synthesis efficiency is significantly better in the lesion-containing template (Fig. 5C, bottom of each panel) (*t* test; $P < 0.05$). Thus, it seems that both DinB and DinB(F292Y) prefer lesion-containing templates over undamaged DNA (Fig. 5C), though for DinB(F292Y) this preference is mostly evident at the undiluted protein concentration (lane 10) (*t* test; $P < 0.05$). Unlike DinB or DinB(F292Y), the DinB(V7G) variant has *in vitro* activity, but it seems to lack a significant preference for the lesion-containing template (Fig. 5C) (*t* test; $P > 0.05$). The V7 amino acid is in close proximity to the catalytic pocket of DinB, and the V7G amino acid substitution may alter the preference of DinB for lesion-containing DNA. A DinB *in vitro* preference for an N^2-dG-containing template has been previously observed (13). The preference for lesion-containing DNA provides additional evidence that lesions might target DinB to the DNA and it is consistent with the EMSA (Fig. 1C).

It is conceivable, though unlikely given the functional *in vivo* and *in vitro* data, that the F292Y or V7G suppressor mutations disrupted DinB's structure. To examine this possibility, we used circular dichroism spectroscopy to determine the secondary structure of DinB(F292Y). We found that the change from the nonpolar F to the polar Y does not alter the secondary structure (see Fig. S8 in the supplemental material) of DinB. This is in agreement with the *in vitro* and *in vivo* data suggesting that it retains both catalytic and TLS activity (Fig. 5).

Because the F292Y and V7G mutations suppressed the DinB-mediated MMS sensitivity in the *dnaE915* strain, we sought to determine if these mutations would suppress the survival loss associated with the overproduction of DinB in a *dnaE*$^+$ strain as well. This would demonstrate that they are not simply artifacts of a strain (*dnaE915* strain) with a defective replication complex. We constructed pBAD18 arabinose-inducible plasmids bearing either *dinB*$^+$, *dinB*(*D103N*), *dinB*(*F292Y*), or *dinB*(*V7G*) and introduced them into both *dnaE*$^+$ Δ*dinB* and *dnaE915* Δ*dinB* strains. We find that overall the *dnaE915* strain is ~100-fold more sensi-

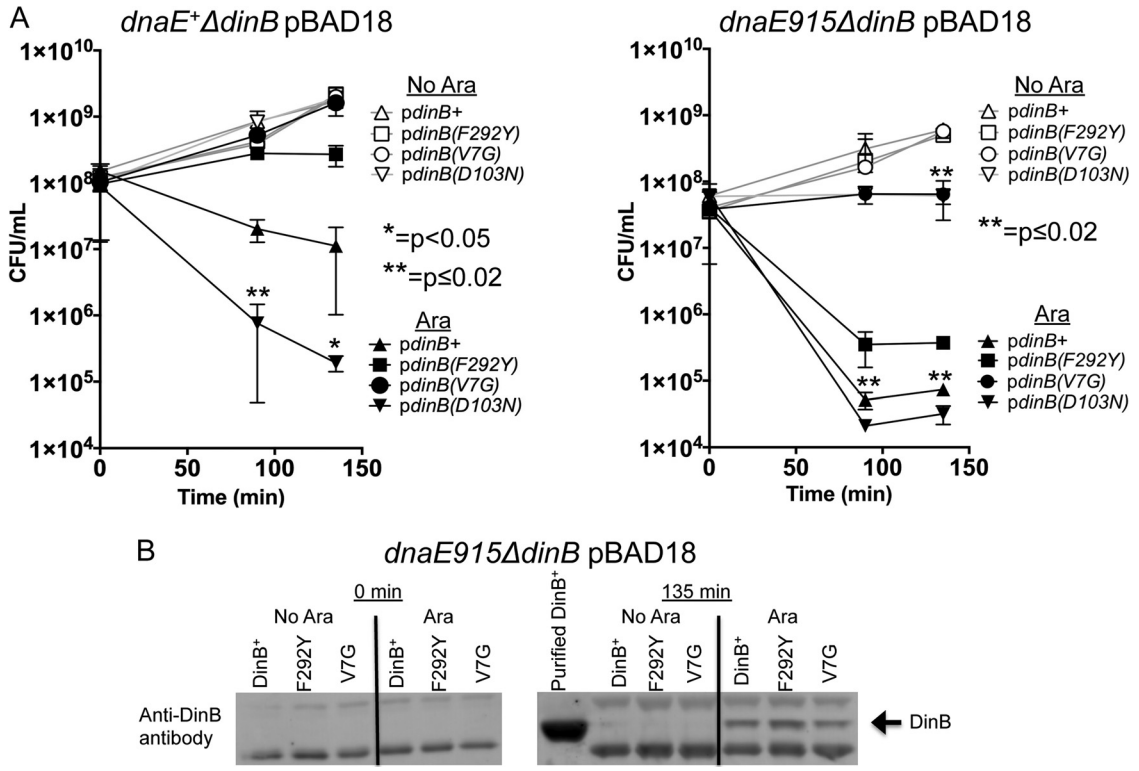

FIG 6 The *dinB*(*F292Y*) and *dinB*(*V7G*) alleles also suppress DinB-mediated overexpression toxicity in *dnaE*$^+$ cells. (A) Samples were collected at the indicated times from cultures with (filled symbols) or without (empty symbols) arabinose induction. Overproduction of wild-type DinB (filled triangle) or catalytically inactive DinB(D103N) (filled inverted triangle) is toxic to both *dnaE*$^+$ and *dnaE915* strains. The DinB(F292Y) (squares) and DinB(V7G) (circles) variants suppress DinB-mediated toxicity, compared to DinB (triangles) in both *dnaE*$^+$ and *dnaE915* strains. Error bars represent the standard deviations of the means from at least 3 independent isolates. (B) *dnaE915* strains overexpress DinB, DinB(F292Y), or DinB(V7G) at similar levels. Immunoblotting (as described in Materials and Methods) assessed whether DinB and DinB(F292Y) or DinB(V7G) are equally translated. In uninduced cultures, DinB and its variants are undetectable. Purified DinB protein (750 ng) was used for sizing purposes. Samples were loaded with comparable protein concentrations as shown by cross-reactive bands.

tive to DinB overexpression than the *dnaE*$^+$ strain (Fig. 6A, right panel). Notably, *dnaE*$^+$ is more sensitive to DinB(D103N) overexpression than DinB (Fig. 6A). This is an additional example of increased DinB(D103N) toxicity compared to DinB, similar to what is found when they are expressed from their native promoter in low-copy-number plasmids (Fig. 2 and 3).

We find that the *dinB*(*V7G*) or *dinB*(*F292Y*) alleles suppress the DinB overproduction toxicity in the *dnaE*$^+$ Δ*dinB* strain (Fig. 6A, left panel). In fact, cells overexpressing DinB(V7G) proliferate similarly to the uninduced cells (Fig. 6A, left panel). This toxicity is also suppressed in the *dnaE915* Δ*dinB* strain with DinB(V7G), and although overexpression of DinB(F292Y) results in CFU loss compared to the uninduced control, DinB(F292Y)'s toxicity is significantly less than that of native DinB (Fig. 6A, right panel). These two derivatives, DinB(F292Y) and DinB(V7G), are detected by immunoblotting at levels similar to DinB in *dnaE915* Δ*dinB* cells (Fig. 6B). We estimate that the concentration of DinB protein in cells is approximately 100-fold higher (~300 μM) than in a fully SOS induced cell (~3 μM [4]). Thus, suppression of DinB toxicity in this assay is not due to variations in protein levels.

DISCUSSION

The experiments in this study were undertaken to examine whether we could gain further insights into mechanisms underlying the DinB-mediated survival loss upon overexpression (17, 18). We used alleles of DNA Pol IV (DinB) (Table 3) and the *dnaE915* allele (21, 22), an antimutator allele that reduces DinB-dependent mutations (23, 24). Thus, we hypothesized that genetic interactions between *dnaE915* and *dinB* variants should result in detectable changes in DinB-dependent phenotypes.

Remarkably, we find that *dnaE915* cells carrying either a chromosomal catalytically deficient *dinB*(*D103N*) allele or plasmid-borne *dinB*$^+$ under the control of its own promoter are sensitized to treatment with MMS, an agent that forms 3-meA lesions (Fig. 1 and 2). Moreover, here we show that DinB has a preference for DNA primers/templates containing a 3-meA lesion analogue (Fig. 1C and 5C), a previously unknown characteristic of DinB. This is consistent with previous data (13) and suggests that lesions might help target DinB to the DNA *in vivo* and in turn elevate its local concentration above a threshold necessary to effect survival loss. Thus, it makes sense that DinB overexpression is required in the absence of DNA damage treatment to observe survival loss or DinB-mediated toxicity as observed here (Fig. 6) and in previous reports (18).

Notably, in the absence of DNA damage treatment we find an antagonistic genetic interaction between *dnaE915* and the catalytically inactive *dinB*(*D103N*) allele expressed from its own promoter on a low-copy-number plasmid. This synthetic sickness phenotype is manifested both as aberrant colony morphology

TABLE 3 *dinB* alleles and phenotypes

Allele	Phenotype[j] of strain carrying:									
	dnaE$^+$					*dnaE915*				
	On chromosome and treated with:		On low-copy-no. plasmid and treated with:			On chromosome and treated with:		On low-copy-no. plasmid and treated with:		
	NFZ[h]	MMS[i]	NFZ	MMS	OE[g]	NFZ	MMS	NFZ	MMS	OE
Δ*dinB*	S[a]	S[b]	S[a,e]	S[b,e]	—[f]	S	S	—	—	—
dinB$^+$	R[a]	R[b]	R[a]	R[b]	T[c]	R	R	R	HS	T
dinB(*D103N*)	S[d]	S[d]	HS[a]	HS[d]	T	HS	HS	HS	HS	T
dinB(*D103N*Δβ)	ND	ND	S[d]	S[d]	ND	ND	ND	S	S	ND
dinB(*V288G*)	ND	ND	S	S	ND	ND	ND	S	S	ND
dinB(*F292Y*)	ND	ND	R	R	RT	ND	ND	R	S	RT
dinB(*V7G*)	ND	ND	R	R	RT	ND	ND	R	R	RT

[a] See reference 13.
[b] See reference 16.
[c] See reference 18.
[d] See reference 14.
[e] Vector alone.
[f] —, not applicable.
[g] OE, overexpressed.
[h] NFZ, nitrofurazone.
[i] MMS, methyl methanesulfonate.
[j] R, resistant, full growth; S, sensitive, at least 10-fold-fewer CFU than *dinB*$^+$ strain; HS, hypersensitive, fewer CFU than Δ*dinB* strain or Δ*dinB* strain with vector; T, toxic, overexpression results in at least 100-fold-fewer CFU than strain with chromosomal *dinB*$^+$; RT, reduced toxicity compared to *dinB*$^+$; ND, not done.

(Fig. 3A) and the inability to reach saturation in rich medium (Fig. 3B). Since DinB(D103N) is catalytically inactive, this phenotype is likely the result of protein-protein or protein-DNA interactions at the replication fork. We infer that the observed synthetic sickness is due to replication stress because the SOS gene network is induced in a large fraction (~25 to 40%) of these cells in the absence of exogenous sources of DNA damage (Fig. 3A and C). This phenotype is similar to what has been reported with cells carrying an identical plasmid-borne *dinB*(*D103N*) allele and an allele of *dnaN* encoding a temperature-sensitive variant of the β-clamp that is thought to enhance polymerase switching between DinB and a stalled Pol IIIα (42). This furthers our hypothesis that the antagonistic genetic interaction between plasmid-borne *dinB*(*D103N*) and *dnaE915* is the result of an interruption of normal DNA replication.

Although the fact that the *dnaE915* allele is an antimutator and also sensitizes cells to DinB might seem counterintuitive, both phenotypes are likely the result of Pol IIIα(915) dissociating from the replication fork more easily than native Pol IIIα. It has been suggested that this dissociation allows DNA Pol II to proofread and correct mispaired nucleotides, while simultaneously excluding DinB from extending in an error-prone manner, thus reducing mutagenesis (24). When the concentration of DinB is increased at the replication fork via overproduction or DNA damage recruitment, DinB could similarly displace Pol IIIα(915) more easily than Pol IIIα and stall DNA replication.

Our genetic analysis has permitted the identification of several intragenic *dinB* mutations (Fig. 4) that rescue both *dnaE915* and *dnaE*$^+$ strains from DinB-dependent survival loss (Fig. 6; see Fig. S6 and S7 in the supplemental material) suggesting that the *dinB* alleles we have discovered are biologically relevant. We noticed that many of these mutations are localized to two areas of DinB (Fig. 4 and Table 2), suggesting that these are important for interactions between DinB and other molecules. In addition to the novel active DinB derivatives we discovered and analyzed (Fig. 5 and 6 and Table 2), our genetic system also selected for base pair substitution alleles that render DinB nonfunctional [the *dinB72* allele encoding DinB(V288G)] or mutations resulting in DinB derivatives that may disrupt interactions with the β-clamp processivity factor [DinB(L307Q), DinB(L349P), and DinB(L351S)] (36, 38). It is plausible that some of the mutations identified in these areas could spatially affect distant portions of the DinB protein and in this manner affect the protein's structure and/or stability, though we have no evidence for this in the present report. Data from our investigation do not allow us to identify specific interacting partners; however, future biochemical studies will address these questions.

From our findings we hypothesize that TLS and DinB-dependent survival loss are distinct mechanisms that share many of the same requirements and factors. DinB(V7G) and DinB(F292Y) both retain catalytic activity (Fig. 5) but do not effect overexpression toxicity in *dnaE*$^+$ cells (Fig. 6A), demonstrating that these two DinB activities can be genetically separated. Some molecular interactions, such as those with the β-clamp processivity factor, are required for both TLS and survival loss; however, this is likely because both TLS and survival loss require DinB to be localized to the replication fork.

The *dnaE915* genetic system that we have utilized allows for the identification of areas of DinB that are important for survival loss upon DNA damage treatment, which are in turn likely important for other cellular processes, such as interplay between DNA polymerases.

ACKNOWLEDGMENTS

This work was supported by NIGMS RO1GM088230, awarded to V.G.G. R.W.B. is currently supported at the Forsyth Institute by a training

grant from the National Institute of Dental and Craniofacial Research, T32 DE007327.

R.W.B. thanks the ASM Scientific Writing and Publishing Institute for the invaluable experience gained at the institute. We thank the Lewis Lab at Northeastern University, the Rosenberg Lab at Baylor College of Medicine, the Sandler Lab at the University of Massachusetts at Amherst, and the Beckwith Lab at Harvard Medical School for strains and plasmids. We also thank the Cram and Chai Labs at Northeastern University for equipment. The anti-DinB antibody was a kind gift from Masami Yamada and Takehiko Nohmi at the National Institute of Health Sciences in Japan. We also appreciate the help of two Northeastern University undergraduate students, Lola Galczynski and Kathy Fatovic, for isolating suppressor mutations and cell counting in the microscopy experiments, respectively.

REFERENCES

1. **Friedberg EC, Walker GC, Siede W, Wood RD, Schultz RA, Ellenberger T.** 2006. DNA repair and mutagenesis, 2nd ed. ASM Press, Washington, DC.
2. **Courcelle J, Khodursky A, Peter B, Brown PO, Hanawalt PC.** 2001. Comparative gene expression profiles following UV exposure in wild-type and SOS-deficient *Escherichia coli*. Genetics **158:**41–64.
3. **Khil PP, Camerini-Otero RD.** 2002. Over 1000 genes are involved in the DNA damage response of *Escherichia coli*. Mol. Microbiol. **44:**89–105. http://dx.doi.org/10.1046/j.1365-2958.2002.02878.x.
4. **Nohmi T.** 2006. Environmental stress and lesion-bypass DNA polymerases. Annu. Rev. Microbiol. **60:**231–253. http://dx.doi.org/10.1146/annurev.micro.60.080805.142238.
5. **Petrosino JF, Galhardo RS, Morales LD, Rosenberg SM.** 2009. Stress-induced beta-lactam antibiotic resistance mutation and sequences of stationary-phase mutations in the *Escherichia coli* chromosome. J. Bacteriol. **191:**5881–5889. http://dx.doi.org/10.1128/JB.00732-09.
6. **Norton MD, Spilkia AJ, Godoy VG.** 2013. Antibiotic resistance acquired through a DNA damage-inducible response in *Acinetobacter baumannii*. J. Bacteriol. **195:**1335–1345. http://dx.doi.org/10.1128/JB.02176-12.
7. **Cirz RT, Chin JK, Andes DR, de Crecy-Lagard V, Craig WA, Romesberg FE.** 2005. Inhibition of mutation and combating the evolution of antibiotic resistance. PLoS Biol. **3:**e176. http://dx.doi.org/10.1371/journal.pbio.0030176.
8. **Cirz RT, Romesberg FE.** 2006. Induction and inhibition of ciprofloxacin resistance-conferring mutations in hypermutator bacteria. Antimicrob. Agents Chemother. **50:**220–225. http://dx.doi.org/10.1128/AAC.50.1.220-225.2006.
9. **Stallons LJ, McGregor WG.** 2010. Translesion synthesis polymerases in the prevention and promotion of carcinogenesis. J. Nucleic Acids. **2010:**643857. http://dx.doi.org/10.4061/2010/643857.
10. **Waters LS, Minesinger BK, Wiltrout ME, D'Souza S, Woodruff RV, Walker GC.** 2009. Eukaryotic translesion polymerases and their roles and regulation in DNA damage tolerance. Microbiol. Mol. Biol. Rev. **73:**134–154. http://dx.doi.org/10.1128/MMBR.00034-08.
11. **Pillaire MJ, Selves J, Gordien K, Gourraud PA, Gentil C, Danjoux M, Do C, Negre V, Bieth A, Guimbaud R, Trouche D, Pasero P, Mechali M, Hoffmann JS, Cazaux C.** 2010. A 'DNA replication' signature of progression and negative outcome in colorectal cancer. Oncogene **29:**876–887. http://dx.doi.org/10.1038/onc.2009.378.
12. **Betous R, Rey L, Wang G, Pillaire MJ, Puget N, Selves J, Biard DS, Shin-ya K, Vasquez KM, Cazaux C, Hoffmann JS.** 2009. Role of TLS DNA polymerases eta and kappa in processing naturally occurring structured DNA in human cells. Mol. Carcinog. **48:**369–378. http://dx.doi.org/10.1002/mc.20509.
13. **Jarosz DF, Godoy VG, Delaney JC, Essigmann JM, Walker GC.** 2006. A single amino acid governs enhanced activity of DinB DNA polymerases on damaged templates. Nature **439:**225–228. http://dx.doi.org/10.1038/nature04318.
14. **Benson RW, Norton MD, Lin I, Du Comb WS, Godoy VG.** 2011. An active site aromatic triad in *Escherichia coli* DNA Pol IV coordinates cell survival and mutagenesis in different DNA damaging agents. PLoS One **6:**e19944. http://dx.doi.org/10.1371/journal.pone.0019944.
15. **Jarosz DF, Cohen SE, Delaney JC, Essigmann JM, Walker GC.** 2009. A DinB variant reveals diverse physiological consequences of incomplete TLS extension by a Y-family DNA polymerase. Proc. Natl. Acad. Sci. U. S. A. **106:**21137–21142. http://dx.doi.org/10.1073/pnas.0907257106.
16. **Bjedov I, Dasgupta CN, Slade D, Le Blastier S, Selva M, Matic I.** 2007. Involvement of *Escherichia coli* DNA polymerase IV in tolerance of cytotoxic alkylating DNA lesions *in vivo*. Genetics **176:**1431–1440. http://dx.doi.org/10.1534/genetics.107.072405.
17. **Foti JJ, Devadoss B, Winkler JA, Collins JJ, Walker GC.** 2012. Oxidation of the guanine nucleotide pool underlies cell death by bactericidal antibiotics. Science **336:**315–319. http://dx.doi.org/10.1126/science.1219192.
18. **Uchida K, Furukohri A, Shinozaki Y, Mori T, Ogawara D, Kanaya S, Nohmi T, Maki H, Akiyama M.** 2008. Overproduction of *Escherichia coli* DNA polymerase DinB (Pol IV) inhibits replication fork progression and is lethal. Mol. Microbiol. **70:**608–622. http://dx.doi.org/10.1111/j.1365-2958.2008.06423.x.
19. **Furukohri A, Goodman MF, Maki H.** 2008. A dynamic polymerase exchange with *Escherichia coli* DNA polymerase IV replacing DNA polymerase III on the sliding clamp. J. Biol. Chem. **283:**11260–11269. http://dx.doi.org/10.1074/jbc.M709689200.
20. **Indiani C, Langston LD, Yurieva O, Goodman MF, O'Donnell M.** 2009. Translesion DNA polymerases remodel the replisome and alter the speed of the replicative helicase. Proc. Natl. Acad. Sci. U. S. A. **106:**6031–6038. http://dx.doi.org/10.1073/pnas.0901403106.
21. **Fijalkowska IJ, Schaaper RM.** 1993. Antimutator mutations in the alpha subunit of *Escherichia coli* DNA polymerase III: identification of the responsible mutations and alignment with other DNA polymerases. Genetics **134:**1039–1044.
22. **Fijalkowska IJ, Dunn RL, Schaaper RM.** 1993. Mutants of *Escherichia coli* with increased fidelity of DNA replication. Genetics **134:**1023–1030.
23. **Hastings PJ, Hersh MN, Thornton PC, Fonville NC, Slack A, Frisch RL, Ray MP, Harris RS, Leal SM, Rosenberg SM.** 2010. Competition of *Escherichia coli* DNA polymerases I, II and III with DNA Pol IV in stressed cells. PLoS One **5:**e10862. http://dx.doi.org/10.1371/journal.pone.0010862.
24. **Banach-Orlowska M, Fijalkowska IJ, Schaaper RM, Jonczyk P.** 2005. DNA polymerase II as a fidelity factor in chromosomal DNA synthesis in *Escherichia coli*. Mol. Microbiol. **58:**61–70. http://dx.doi.org/10.1111/j.1365-2958.2005.04805.x.
25. **Cairns J, Foster PL.** 1991. Adaptive reversion of a frameshift mutation in *Escherichia coli*. Genetics **128:**695–701.
26. **Blattner FR, Plunkett G, III, Bloch CA, Perna NT, Burland V, Riley M, Collado-Vides J, Glasner JD, Rode CK, Mayhew GF, Gregor J, Davis NW, Kirkpatrick HA, Goeden MA, Rose DJ, Mau B, Shao Y.** 1997. The complete genome sequence of *Escherichia coli* K-12. Science **277:**1453–1462. http://dx.doi.org/10.1126/science.277.5331.1453.
27. **Wagner J, Gruz P, Kim SR, Yamada M, Matsui K, Fuchs RP, Nohmi T.** 1999. The *dinB* gene encodes a novel *E. coli* DNA polymerase, DNA pol IV, involved in mutagenesis. Mol. Cell **4:**281–286. http://dx.doi.org/10.1016/S1097-2765(00)80376-7.
28. **Guzman LM, Belin D, Carson MJ, Beckwith J.** 1995. Tight regulation, modulation, and high-level expression by vectors containing the arabinose PBAD promoter. J. Bacteriol. **177:**4121–4130.
29. **Miller JH.** 1992. A short course in bacterial genetics: a laboratory manual and handbook for *Escherichia coli* and related bacteria. Cold Spring Harbor Laboratory Press, Plainview, NY
30. **Plosky BS, Frank EG, Berry DA, Vennall GP, McDonald JP, Woodgate R.** 2008. Eukaryotic Y-family polymerases bypass a 3-methyl-2′-deoxyadenosine analog *in vitro* and methyl methanesulfonate-induced DNA damage *in vivo*. Nucleic Acids Res. **36:**2152–2162. http://dx.doi.org/10.1093/nar/gkn058.
31. **McCool JD, Long E, Petrosino JF, Sandler HA, Rosenberg SM, Sandler SJ.** 2004. Measurement of SOS expression in individual *Escherichia coli* K-12 cells using fluorescence microscopy. Mol. Microbiol. **53:**1343–1357. http://dx.doi.org/10.1111/j.1365-2958.2004.04225.x.
32. **Cafarelli TM, Rands TJ, Benson RW, Rudnicki PA, Lin I, Godoy VG.** 2013. A single residue unique to DinB-like proteins limits formation of the Pol IV multiprotein complex in *Escherichia coli*. J. Bacteriol. **195:**1179–1193. http://dx.doi.org/10.1128/JB.01349-12.
33. **Benson RW, Cafarelli TM, Godoy VG.** 2011. SOE-LRed: a simple and time-efficient method to localize genes with point mutations onto the *Escherichia coli* chromosome. J. Microbiol. Methods **84:**479–481. http://dx.doi.org/10.1016/j.mimet.2010.12.020.
34. **Kim SR, Maenhaut-Michel G, Yamada M, Yamamoto Y, Matsui K, Sofuni T, Nohmi T, Ohmori H.** 1997. Multiple pathways for SOS-induced mutagenesis in *Escherichia coli*: an overexpression of *dinB/dinP* results in strongly enhancing mutagenesis in the absence of any exogenous

treatment to damage DNA. Proc. Natl. Acad. Sci. U. S. A. **94:**13792–13797. http://dx.doi.org/10.1073/pnas.94.25.13792.
35. **Guarente L.** 1993. Synthetic enhancement in gene interaction: a genetic tool come of age. Trends Genet. **9:**362–366. http://dx.doi.org/10.1016/0168-9525(93)90042-G.
36. **Wagner J, Fujii S, Gruz P, Nohmi T, Fuchs RP.** 2000. The beta clamp targets DNA polymerase IV to DNA and strongly increases its processivity. EMBO Rep. **1:**484–488. http://dx.doi.org/10.1093/embo-reports/kvd109.
37. **Bunting KA, Roe SM, Pearl LH.** 2003. Structural basis for recruitment of translesion DNA polymerase Pol IV/DinB to the beta-clamp. EMBO J. **22:**5883–5892. http://dx.doi.org/10.1093/emboj/cdg568.
38. **Heltzel JM, Maul RW, Scouten Ponticelli SK, Sutton MD.** 2009. A model for DNA polymerase switching involving a single cleft and the rim of the sliding clamp. Proc. Natl. Acad. Sci. U. S. A. **106:**12664–12669. http://dx.doi.org/10.1073/pnas.0903460106.
39. **Friedberg EC, Fischhaber PL, Kisker C.** 2001. Error-prone DNA polymerases: novel structures and the benefits of infidelity. Cell **107:**9–12. http://dx.doi.org/10.1016/S0092-8674(01)00509-8.
40. **Pham PT, Olson MW, McHenry CS, Schaaper RM.** 1998. The base substitution and frameshift fidelity of *Escherichia coli* DNA polymerase III holoenzyme in vitro. J. Biol. Chem. **273:**23575–23584. http://dx.doi.org/10.1074/jbc.273.36.23575.
41. **Cafarelli TM, Rands TJ, Godoy VG.** 2014. The DinB*RecA complex of *Escherichia coli* mediates an efficient and high-fidelity response to ubiquitous alkylation lesions. Environ. Mol. Mutagen. **55:**92–102. http://dx.doi.org/10.1002/em.21826.
42. **Heltzel JM, Maul RW, Wolff DW, Sutton MD.** 2012. *Escherichia coli* DNA polymerase IV (Pol IV), but not Pol II, dynamically switches with a stalled Pol III* replicase. J. Bacteriol. **194:**3589–3600. http://dx.doi.org/10.1128/JB.00520-12.